Stem Cell Reports
Report
OPEN ACCESS

Epigenetic Aberrations Are Not Specific to Transcription Factor-Mediated Reprogramming

Ulf Tiemann,[1] Guangming Wu,[2] Adele Gabriele Marthaler,[2] Hans Robert Schöler,[2,3,*] and Natalia Tapia[1,*]
[1]Medical Faculty, Heinrich Heine University, Moorenstraße 5, 40225 Düsseldorf, Germany
[2]Department of Cell and Developmental Biology, Max Planck Institute for Molecular Biomedicine, Röntgenstraße 20, 48149 Münster, Germany
[3]Medical Faculty, University of Münster, Domagkstraße 3, 48149 Münster, Germany
*Correspondence: natalia.tapia@med.uni-duesseldorf.de (N.T.), office@mpi-muenster.mpg.de (H.R.S.)
http://dx.doi.org/10.1016/j.stemcr.2015.11.007

SUMMARY

Somatic cells can be reprogrammed to pluripotency using different methods. In comparison with pluripotent cells obtained through somatic nuclear transfer, induced pluripotent stem cells (iPSCs) exhibit a higher number of epigenetic errors. Furthermore, most of these abnormalities have been described to be intrinsic to the iPSC technology. Here, we investigate whether the aberrant epigenetic patterns detected in iPSCs are specific to transcription factor-mediated reprogramming. We used germline stem cells (GSCs), which are the only adult cell type that can be converted into pluripotent cells (gPSCs) under defined culture conditions, and compared GSC-derived iPSCs and gPSCs at the transcriptional and epigenetic level. Our results show that both reprogramming methods generate indistinguishable states of pluripotency. GSC-derived iPSCs and gPSCs retained similar levels of donor cell-type memory and exhibited comparable numbers of reprogramming errors. Therefore, our study demonstrates that the epigenetic abnormalities detected in iPSCs are not specific to transcription factor-mediated reprogramming.

INTRODUCTION

Previous studies have reported that induced pluripotent stem cells (iPSCs) retain epigenetic traits of the tissue of origin and accumulate DNA methylation errors during the reprogramming process (Kim et al., 2010; Ma et al., 2014). However, whether these epigenetic abnormalities are a consequence of cellular reprogramming per se or are specific to the iPSC technology remains controversial. A previous study has shown that most of the abnormalities found in iPSCs are introduced during the reprogramming process (Ma et al., 2014). Indeed, iPSCs exhibit more aberrations than pluripotent cells obtained through somatic cell nuclear transfer (SCNT) (Ma et al., 2014). In this study, we used a third reprogramming method to investigate whether iPSC epigenetic errors are a consequence of the ectopic expression of transcription factors. Germline stem cells (GSCs) are the only adult cell type that can be converted into pluripotent stem cells, termed germline pluripotent stem cells (gPSCs), under specific culture conditions (Ko et al., 2009). Thus, we compared GSC-derived iPSCs with gPSCs at the transcriptional and epigenetic level. Global gene expression and genome-wide DNA methylation analysis confirmed that GSC-derived iPSCs and gPSCs exhibit similar levels of donor memory and de novo reprogramming errors. Therefore, our results indicate that epigenetic aberrations are not specific to transcription factor-mediated reprogramming.

RESULTS

Conversion of GSCs to Pluripotency Using Two Different Reprogramming Methods

We derived two GSC lines, named GSC #1 and #2, from mice containing an *Oct4*-GFP reporter transgene (Yoshimizu et al., 1999). Next, we reprogrammed both GSC lines to pluripotency using two different methods (Figure 1A). First, doxycycline-inducible lentiviruses coding for *Oct4*, *Sox2*, *Kfl4*, and *Myc*, together with a reverse tetracycline transactivator (Brambrink et al., 2008), were used to generate iPSCs from both GSC lines. *Oct4*-GFP-positive colonies emerged 5–8 days after transgene induction. Although a previous study reported the inability to generate GSC-derived iPSCs using constitutively expressed lentiviruses (Morimoto et al., 2012), we were able to reprogram GSCs into iPSCs using inducible lentiviruses (for details see Supplemental Experimental Procedures). In parallel, iPSCs were generated from fibroblasts (Fib) from the same mouse line and following the same procedure. Interestingly, Fib-iPSC colonies were not observed until 10–20 days after doxycycline induction, demonstrating that GSCs are reprogrammed significantly faster than other somatic cell types. As previously reported, the stoichiometry of the reprogramming factors influences the iPSC generation rate. Indeed, a high relative level of both *Oct4* and *Klf4* combined with a low relative level of *Sox2* and *Myc* has been described to increase the reprogramming efficiency (Tiemann et al., 2011). Accordingly, GSCs were

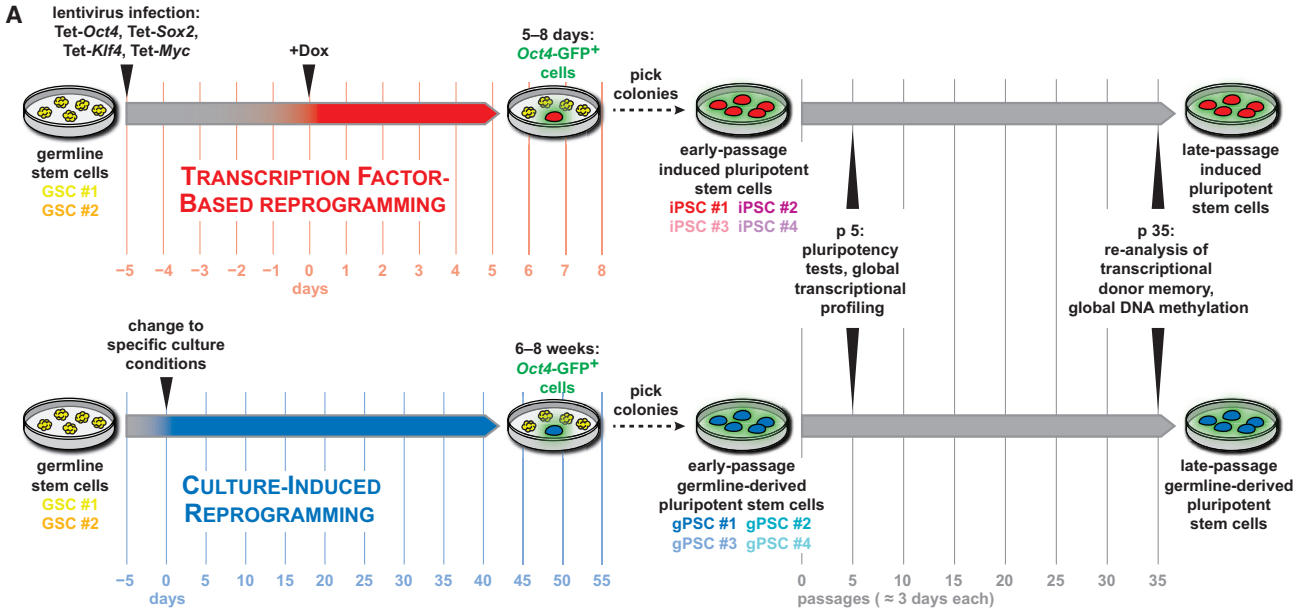

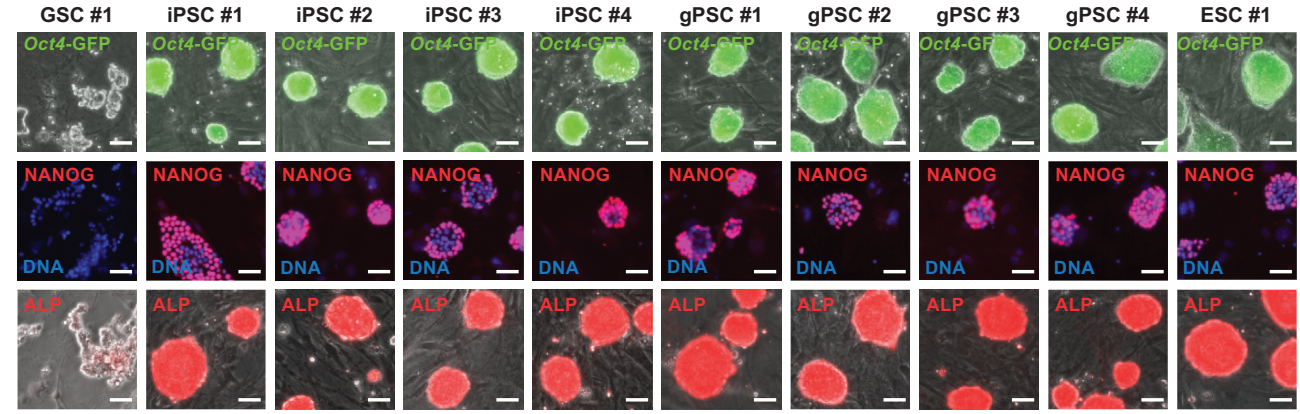

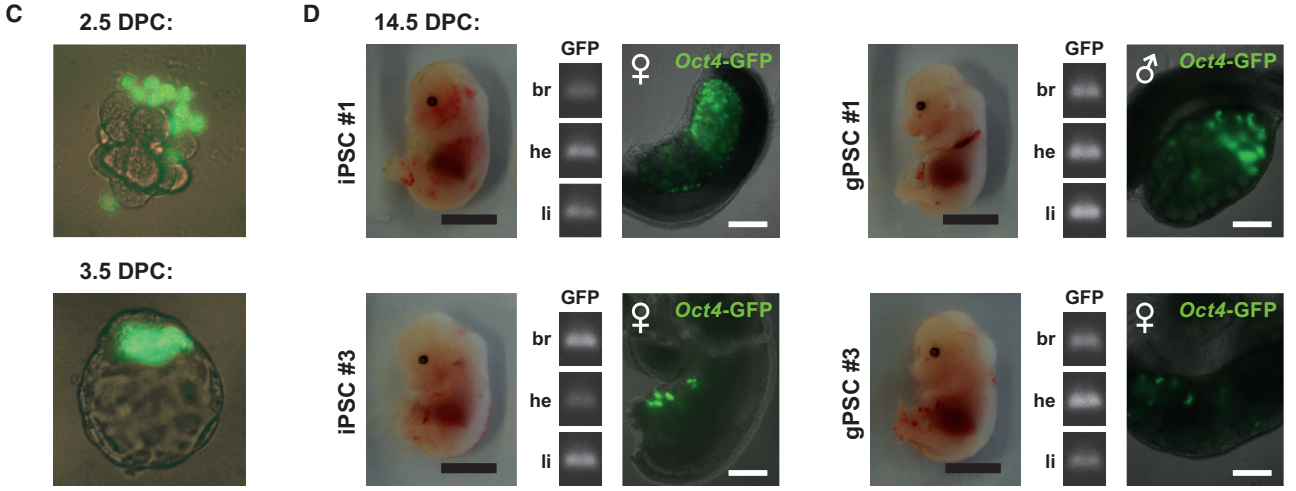

(legend on next page)

reprogrammed into iPSCs 5-fold more efficiently after using higher ratios of both *Oct4* and *Klf4*, whereas a lower ratio of these two factors completely prevented iPSC induction (Figure S1A). Four tetracycline-independent, *Oct4*-GFP-positive iPSC cell lines were established and termed iPSC #1, #2, #3, and #4 (Figure 1A). Integration of all four lentiviral transgenes was detected in all generated iPSC lines using PCR-based genotyping (Figure S1B).

Second, GSC lines #1 and #2 were reprogrammed into gPSCs under specific culture conditions, as previously reported (Ko et al., 2010). *Oct4*-GFP-positive colonies were observed after 6–8 weeks (Figure 1A). Four gPSC lines were derived from single-cell colonies and named gPSC #1, #2, #3, and #4 (Figure 1A). As expected, we did not detect any lentiviral transgenes in the generated gPSC lines (Figure S1B). In total, eight different reprogrammed cell lines corresponding to four independent iPSC and gPSC clones were subsequently analyzed at an early stage (passage 5) and late stage (passage 35) after reprogramming (Figure 1A).

Next, we characterized the pluripotency of the reprogrammed iPSC and gPSC lines. To this end, the presence of several pluripotency-specific proteins was assessed. In contrast to the parental GSCs, the generated iPSC and gPSC lines strongly expressed the *Oct4*-GFP transgene and stained positive for the pluripotent markers NANOG and alkaline phosphatase (Figure 1B). In addition, the transcriptional levels of the endogenous pluripotent markers *Oct4*, *Sox2*, *Nanog*, and *Esrrb* were analyzed by qRT-PCR (Figure S2A). All iPSC and gPSC clones exhibited expression levels similar to those of embryonic stem cells (ESCs) and different from those of the initial GSC population, demonstrating a successful reprogramming to pluripotency. Furthermore, all iPSC and gPSC lines showed a normal karyotype (Figure S2B). Finally, we investigated the developmental potential of the generated iPSC and gPSC lines. After undirected differentiation using embryoid bodies, all cell lines stained positive for TUBB3 (ectoderm), ACTA2 (mesoderm), and SOX17 (endoderm), thus proving their ability to differentiate in vitro into cell types of all three germ layers (Figure S2C). Moreover, iPSC and gPSC lines were aggregated with morula-stage embryos to assess their potential to generate chimeric embryos in vivo. The following day, *Oct4*-GFP-positive cells had integrated into the blastocyst inner cell mass (Figure 1C). All tested iPSC and gPSC lines were able to contribute to the germline as shown by the presence of *Oct4*-GFP-positive cells in the gonads of embryos 14.5 days post coitum (DPC). Furthermore, *Oct4*-GFP genotyping revealed that iPSCs and gPSCs were able to contribute to brain (ectoderm), heart (mesoderm), and liver (endoderm), indicating their capacity to differentiate into all three germ layers in vivo (Figure 1D). Taken together, these results demonstrate that all analyzed iPSC and gPSC lines are bona fide pluripotent cells.

Global Gene Expression Profiling of iPSCs and gPSCs

To investigate whether the two studied reprogramming methods exhibit different potentials to remodel the initial GSC transcriptional network, we recorded the global gene expression profile of the generated iPSC, gPSC, and control cell lines using microarray analysis. We decided to analyze the reprogrammed cell lines at passage 5, since donor cell-type transcriptional memory in iPSCs has been reported to be predominant at early passages (Polo et al., 2010). A principal-component analysis revealed that all reprogrammed cell lines clustered together with ESCs independently of the reprogramming method (iPSCs versus gPSCs) or the donor cell type (GSCs versus Fib) (Figure 2A). An unsupervised hierarchical clustering further substantiated that the different pluripotent samples could not be distinguished based on the method used for reprogramming. Remarkably, the replicate samples of gPSC #4 and Fib-iPSC that are derived from different cell types and using different techniques could not be separated, further

Figure 1. Conversion of GSCs to Pluripotency Using Two Different Reprogramming Methods

(A) Schematic overview and timeline summarizing cell line derivation and analysis. iPSC and gPSC induction was performed in parallel, but iPSCs emerged at least 5 weeks earlier than gPSCs. In both cases, DNA and RNA were collected at passages 5 and 35 after colony isolation and cell line establishment. At these time points, iPSCs and gPSCs had been cultured for an equivalent period of time. GSC, germline stem cells; iPSC, induced pluripotent stem cells; gPSC, germline-derived pluripotent stem cells; Tet, tetracycline-inducible; Dox, doxycycline; p, passage number.

(B) *Oct4*-GFP reporter fluorescence (green, phase-contrast overlay), immunological staining for NANOG (red, overlay with blue nuclear Hoechst staining), and alkaline phosphatase (ALP) activity assay (red chromogene fluorescence, phase-contrast overlay). ESC, embryonic stem cells; Fib-iPSC, iPSCs derived from fibroblasts. Scale bars, 50 μm.

(C) Representative images of *Oct4*-GFP-positive GSC-derived pluripotent cells after aggregation with a 2.5-DPC morula-stage embryo and after integration into the inner cell mass of a 3.5-DPC blastocyst.

(D) Chimeric embryos (14.5 DPC) showing *Oct4*-GFP-positive contribution in the fetal gonads and positive GFP transgene contribution to several organs (PCR genotyping). br, brain (ectoderm); he, heart (mesoderm); li, liver (endoderm). Black scale bars, 5 mm; white scale bars, 250 μm.

See also Figures S1 and S2, and Tables S2 and S3.

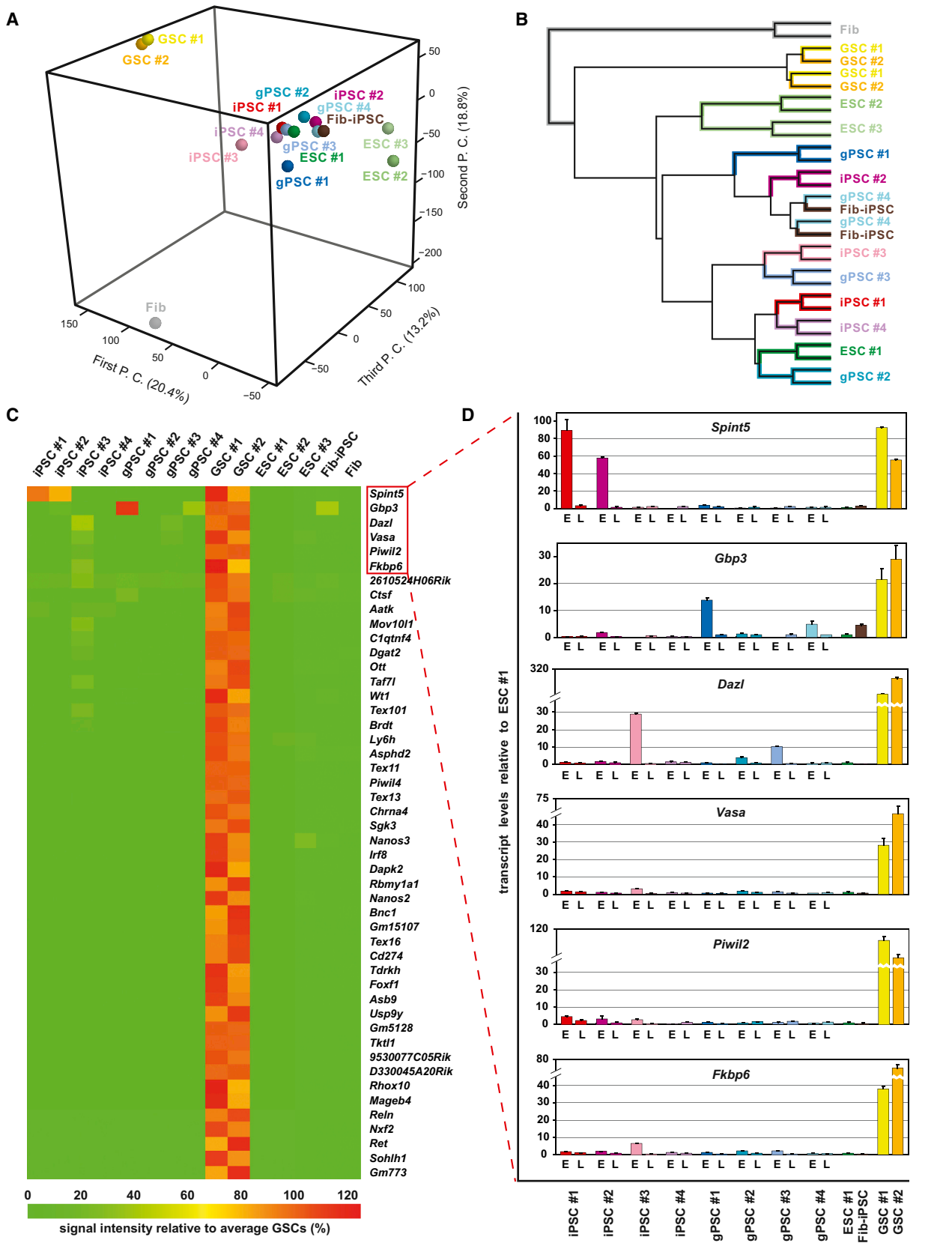

(legend on next page)

demonstrating the similarity of the different pluripotent cell lines (Figure 2B).

Next, we sought to investigate the expression pattern of GSC-specific genes in the iPSC and gPSC lines. To this end, we screened the microarray data for genes that were strongly expressed in both GSC lines but not in ESCs or Fib. Most of these GSC-specific genes were downregulated in all iPSC and gPSC lines, indicating that both reprogramming methods can effectively erase the GSC-specific transcriptional signature (Figure 2C). Only the expression of a few GSC-specific markers such as *Spint5*, *Gbp3*, *Dazl*, *Vasa*, *Piwil2*, and *Fkbp6* could still be detected in some cell lines. These results were confirmed by qRT-PCR (Figure 2D). As previous studies have reported that the initial transcriptional memory in iPSCs can be attenuated after continuous passaging (Polo et al., 2010), we also measured the expression of these GSC-specific markers at a later passage (passage 35) by qRT-PCR. In fact, all reprogrammed cell lines had downregulated the expression of the studied GSC-specific markers at passage 35 (Figure 2D). Therefore, the transcriptomes of both iPSCs and gPSCs were fully reprogrammed at late passage, independently of the method used for reprogramming.

Genome-Wide DNA Methylation Analysis of iPSCs and gPSCs

Several reports have shown that iPSCs with a fully reprogrammed transcriptome can still exhibit epigenetic abnormalities (Kim et al., 2010; Ma et al., 2014). In this context, we performed a genome-wide DNA methylation analysis using reduced-representation bisulfite conversion and subsequent next-generation sequencing (RRBSeq) (Meissner et al., 2005) in two iPSC clones (iPSC #1 and iPSC #2), two gPSC clones (gPSC #1 and gPSC #2), the initial GSC #1 and GSC #2 lines, and three ESC controls (ESC #1 was derived from *Oct4*-GFP transgenic mice, whereas ESC #2 and ESC #3 were derived from a different genetic background) (Table S1). Next, we determined the number of differentially methylated regions (DMRs) for each sample in comparison with the ESC #1 reference sample. Our analysis identified twice as many DMRs in GSCs (average 219,446) as in iPSCs (average 87,028) or gPSCs (average 84,925). Remarkably, we also identified a high number of DMRs between ESC #1 and ESC #2 or ESC #3 (average 206,950). Therefore, the epigenetic differences between reprogrammed cells and ESC #1 were considerably smaller than the epigenetic variation among ESCs from different genetic backgrounds (Figure 3A). On average, 63% of the identified DMRs were located in the context of annotated genes (Figure 3B). In addition, the DMR distribution among the different chromosomes was very similar in all the studied cell lines (Figure 3C).

Furthermore, we analyzed the methylation level of DMRs located within GSC marker genes that are transcriptionally silenced during conversion to pluripotency, as shown in Figure 2C. The gene *Brdt* contained a completely demethylated DMR in GSCs, which was completely remethylated to an ESC-like level in all analyzed iPSC and gPSC lines. In contrast, DMRs associated with other genes such as *Irf8*, *Dapk2*, *Foxf1*, *Wt1*, and *C1qtnf4* exhibited hypomethylation in GSCs but did not fully regain an ESC-like methylation level in all reprogrammed cell lines (Figure 3D). Similarly, DMRs within pluripotency marker genes that are highly methylated in GSCs such as *Zscan10* (Zfp206) and *L1td1* (ECAT11) lost their GSC-like methylation in most but not all reprogrammed cell lines. The genes *Esrrb* and *Cdh1* (E-cadherin) contain DMRs that even remained almost completely methylated in all iPSC and gPSC lines (Figure 3D). Thus, our results demonstrate that reprogrammed cells partially retain donor-like DNA methylation patterns despite their fully ESC-like transcription profiles. Finally, an unsupervised hierarchical clustering including all gene-associated DMRs that are differently methylated between GSCs and ESCs showed that all reprogrammed cell lines cluster together with ESC #1, demonstrating that pluripotent cell lines could be separated based on their genetic background but not based on the reprogramming method (Figure 3E).

We next sought to quantitatively assess how many of the identified DMRs in iPSCs and gPSCs correspond to a

Figure 2. Global Gene Expression Profiling of iPSCs and gPSCs

(A) Principal-component analysis of the global transcriptomes (microarray, passage 5) of iPSCs, gPSCs, and controls. The three principal components (P. C.) that contribute most strongly to the overall variance are shown. Axes are scaled proportionally to the explained portion of variance, as indicated. Two replicates for each clonal cell line were averaged and are represented by a single circle. Fib, fibroblasts.

(B) Dendrogram displaying the results of an unsupervised hierarchical clustering based on the overall correlation among global gene expression profiles. Two technical replicates for each cell line were analyzed independently.

(C) Heatmap showing the expression of GSC-specific marker genes in reprogrammed clonal cell lines. Signal intensities were normalized to the average of the two GSC controls. Red and green colors represent higher and lower gene expression levels in comparison with GSCs, respectively.

(D) Validation of the microarray data presented in (C) by qRT-PCR for selected GSC markers, normalized to ESC #1. E, early passage (p 5); L, late passage (p 35). Error bars indicate SD of the mean (technical replicates, n = 3).

See also Table S3.

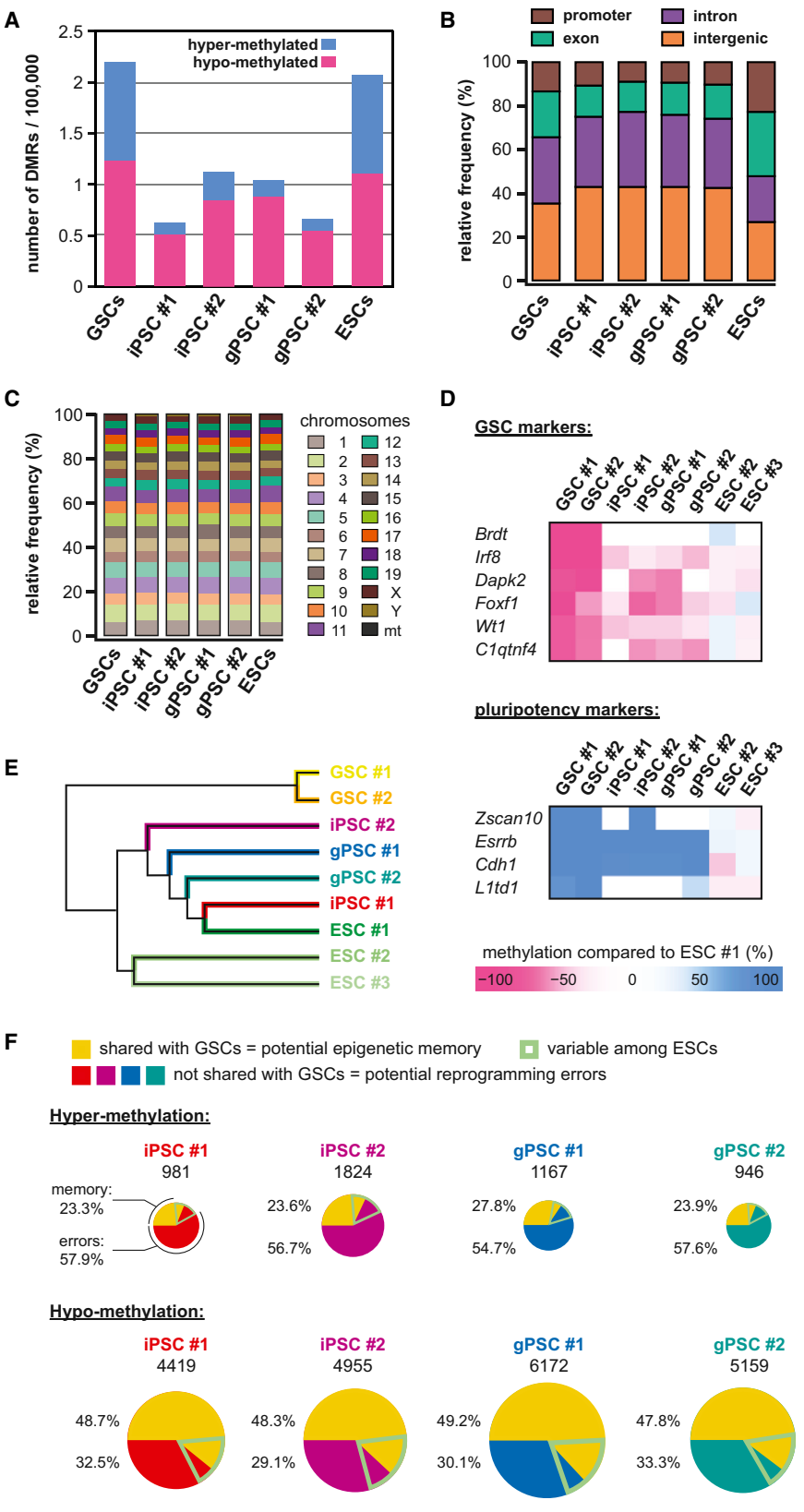

Figure 3. Genome-Wide DNA Methylation Analysis of iPSCs and gPSCs

(A) Differentially methylated regions (DMRs) in the analyzed cell lines. Hyper- and hypomethylated regions exhibit a ≥50% higher or lower CpG methylation rate compared with the ESC #1 control, respectively. GSCs, average of GSC #1 and GSC #2; ESCs, average of ESC #2 and ESC #3.

(B) Mapping of DMRs to different genomic contexts. Relative frequencies of DMRs located in promoters, exons, introns, and outside of annotated genes are shown in comparison with the ESC #1 control (all identified DMRs = 100%).

(C) Chromosomal mapping of DMRs. Relative frequencies of DMRs are shown in comparison with the ESC #1 control (all identified DMRs = 100%). mt, mtDNA.

(D) Sets of GSC-specific markers and pluripotency markers were investigated for the presence of DMRs. Hypo- and hypermethylation relative to the ESC #1 control are displayed by red and blue colors in the heatmaps, respectively.

(E) Dendrogram displaying the results of an unsupervised hierarchical clustering based on hyper- and hypomethylated genes that distinguish GSCs and ESCs.

(F) Numbers of hyper- and hypomethylated DMR-containing genes in the individual iPSC and gPSC clones relative to the ESC #1 control are displayed by differently sized circles. Yellow circular sectors represent DMRs that are also hyper- or hypomethylated in GSC #1 and/or GSC #2 relative to ESC #1, thus corresponding to donor cell-type memory. Green-framed sectors represent DMRs that are also hyper- or hypomethylated in ESC #2 and/or ESC #3 relative to ESC #1, indicating variability among the different ESCs. Red, purple, blue, and cyan sectors represent DMRs that are hyper- or hypomethylated in iPSCs and gPSCs but not in GSCs or ESCs, thus representing reprogramming errors. Percentages of putative donor memory (shared with GSCs but not variable among ESCs) and putative de novo introduced reprogramming errors (not shared with GSCs and not variable among ESCs) are indicated.

See also Table S1.

residual memory of the tissue of origin or to errors de novo introduced during the reprogramming process. First, genes that were hypermethylated or hypomethylated in iPSCs or gPSCs and in at least one GSC line (relative to ESC #1) were considered to represent residual GSC-specific epigenetic memory. Here, we excluded genes differently methylated between ESC #1 and ESC #2 or ESC #3, which can be considered as generally variable in the pluripotent state. Our results indicate that 23.3%–27.8% of the hypermethylated and 48.3%–49.28% of the hypomethylated genes in iPSCs and gPSCs correspond to a donor-specific epigenetic signature (Figure 3F). Second, genes that were hypermethylated or hypomethylated in iPSCs or gPSCs but not in GSCs (relative to ESC #1) were considered to be epigenetic errors de novo introduced during the reprogramming process. Again, genes differently methylated between ESC #1 and ESC #2 or ESC #3 were excluded. Our analysis shows that 54.7%–57.9% of the hypermethylated genes and 29.1%–33.3% of the hypomethylated genes in iPSCs and gPSCs correspond to reprogramming errors (Figure 3F). Overall, these results indicate that hypomethylated DMRs in iPSCs and gPSCs are mainly due to a donor-specific memory, whereas the majority of hypermethylated DMRs probably reflect errors acquired during the reprogramming process. Importantly, the ratio between epigenetic memory and reprogramming errors is very consistent in all analyzed iPSC and gPSC lines, demonstrating that the reprogramming method influences neither the amount of donor cell-type memory nor the de novo introduction of epigenetic aberrations during the acquisition of pluripotency.

DISCUSSION

In this study we have investigated whether epigenetic abnormalities are specific to the transcription factor-mediated reprogramming method. To this end, we took advantage of GSCs, which can be reprogrammed using the iPSC technology or defined culture conditions. Our results show that iPSCs and gPSCs are indistinguishable at the transcriptional and epigenetic levels. In addition, we also tried to reprogram GSCs using SCNT. However, we could not obtain a single blastocyst-stage embryo after reconstructing 1,000 enucleated oocytes with GSC nuclei (data not shown). We excluded the GSC androgenetic imprinting as the cause underlying the SCNT reprogramming failure, since primary spermatocytes have been successfully used in nuclear transfer experiments (Zhao et al., 2010). Hence, further experiments are required to elucidate the inability to reprogram GSCs using nuclear transfer. To date, the reprogramming of stable GSC lines into iPSCs was considered not to be feasible (Morimoto et al., 2012). However, we succeeded in reprogramming GSCs into iPSCs at very low efficiencies after optimizing the transduction protocol. We expected GSCs to be an easily reprogrammable cell type, since GSCs express several pluripotency-related transcripts and exhibit hypomethylation in promoters of pluripotency genes (Imamura et al., 2006). However, GSCs are reluctant to nuclear transfer, and GSC-derived iPSCs can only be generated at very low frequencies. GSCs are the only adult cell type known to express OCT4 protein, albeit at low levels. We speculate that an increase in the OCT4 levels might trigger testicular teratoma formation due to the similarities between iPSC induction and tumor formation (Tapia and Schöler, 2010). Therefore, we hypothesize that GSCs might have a specific mechanism to prevent in vivo reprogramming, which in turn hinders in vitro reprogramming.

Previously, we have shown that fibroblasts can be converted into induced neural stem cells (Kim et al., 2014), which can be reprogrammed to pluripotency in a subsequent step (Marthaler et al., 2013). Our results demonstrated that the pluripotent state could erase the donor cell type transcriptional memory more efficiently than the somatic stem cell state, suggesting that the final developmental state achieved after reprogramming might have a higher impact on the level of residual memory than the reprogramming method itself. Consistently, gPSCs and iPSCs retain the same levels of donor-specific memory since both methods reprogram differentiated cells directly to pluripotency. In contrast, the totipotency state reached during SCNT might explain that SCNT-derived pluripotent cells exhibit lower levels of epigenetic memory than iPSCs (Ma et al., 2014). Recently, iPSC induction has been described to occur in vivo. Interestingly, in vivo reprogrammed iPSCs exhibit totipotency features that are absent in iPSCs generated in vitro (Abad et al., 2013). A genome-wide DNA methylation analysis of these in vivo iPSCs might clarify whether the developmental potential, and not the reprogramming method, is the main player erasing the cell-of-origin epigenetic traits.

The potential use of transcription factor-mediated reprogramming in cell-replacement therapy, disease modeling, and drug discovery can be compromised due to the epigenetic abnormalities described in iPSCs. Human nuclear transfer has been reported as an alternative to Yamanaka's approach (Tachibana et al., 2013). Although both methods introduce comparable levels of de novo coding mutations and imprinting aberrations in the final pluripotent cells (Johannesson et al., 2014), nuclear transfer has been claimed to generate fewer reprogramming errors (Ma et al., 2014). However, SCNT generates autologous pluripotent cells with allogenic mitochondria. Thus, our reprogramming goal should be to reach an SCNT-like pluripotent state using iPSC technology. Our study shows that gPSCs and iPSCs retain similar levels of donor cell-type memory and exhibit comparable numbers of reprogramming errors,

excluding the nonphysiological expression levels of exogenous transcription factors as the cause underlying the differences observed between SCNT ESCs and iPSCs. Therefore, our results indicate that epigenetic aberrations are not specific to transcription factor-mediated reprogramming. Further experiments will need to determine whether the totipotent state generated during nuclear transfer or specific factors present in the oocyte are responsible for the highest reprogramming fidelity observed in SCNT-derived pluripotent cells.

EXPERIMENTAL PROCEDURES

Full details are given in the Supplemental Experimental Procedures.

Cell Line Generation and Culture

Establishment and culture of GSCs, ESCs, and fibroblasts was performed as previously described (Ko et al., 2010, 2012). Animal handling was in accordance with the Max Planck Society animal protection guidelines and the German animal protection laws. GSC-iPSCs were generated by transduction with tetracycline-inducible lentiviruses coding for *Oct4*, *Sox2*, *Klf4*, and *Myc* plus a reverse tetracycline transactivator (Brambrink et al., 2008). Culture-induced reprogramming of GSCs into gPSCs was performed following a previously reported protocol (Ko et al., 2010).

Characterization of Pluripotent Cell Lines

Stainings, karyotyping, and chimera formation were conducted as previously described (Fischedick et al., 2012). In vitro differentiation was performed after embryoid body formation as reported previously (Tiemann et al., 2014). Antibodies are listed in Table S2. The primer sequences for PCR genotyping and SYBR Green qRT-PCR are summarized in Table S3. Microarray analysis (MouseRef 8 v2.0 Expression BeadChips; Illumina) was conducted as previously described (Ko et al., 2011). Next-generation RRBSeq DNA methylation analysis was performed on an Illumina HiSeq platform by GATC Biotech. For details regarding the analysis of global transcriptional and DNA methylation data, see Supplemental Experimental Procedures.

ACCESSION NUMBERS

The NCBI GEO database (http://www.ncbi.nlm.nih.gov/gds) accession number for the microarray and RRBSeq data reported in this paper is GEO: GSE66613.

SUPPLEMENTAL INFORMATION

Supplemental Information includes Supplemental Experimental Procedures, two figures, and three tables and can be found with this article online at http://dx.doi.org/10.1016/j.stemcr.2015.11.007.

AUTHOR CONTRIBUTIONS

U.T., H.R.S., and N.T. conceived the study; U.T. conducted the experiments and analyzed the data; G.W. performed embryo aggregations and nuclear transfer; A.G.M. performed karyotyping; U.T., H.R.S., and N.T. interpreted the results and wrote the manuscript.

ACKNOWLEDGMENTS

We are grateful to Marcos Araúzo-Bravo (BioDonostia Health Research Institute, Spain) for his helpful advice on microarray data analysis. We thank Michele Boiani (Max Planck Institute for Molecular Biomedicine, Germany) and Teruhiko Wakayama (University of Yamanashi, Japan) for their efforts on the SCNT experiments. psPAX2 and pMD2 were gifts from D. Trono. The Max Planck Society is funding H.R.S.'s group, whereas the North-Rhine Westphalia Ministry of Innovation, Science and Research as well as the Heinrich Heine University Düsseldorf are funding N.T.'s Junior Research Group.

Received: March 14, 2015
Revised: November 12, 2015
Accepted: November 18, 2015
Published: December 17, 2015

REFERENCES

Abad, M., Mosteiro, L., Pantoja, C., Canamero, M., Rayon, T., Ors, I., Grana, O., Megias, D., Dominguez, O., Martinez, D., et al. (2013). Reprogramming in vivo produces teratomas and iPS cells with totipotency features. Nature *502*, 340–345.

Brambrink, T., Foreman, R., Welstead, G.G., Lengner, C.J., Wernig, M., Suh, H., and Jaenisch, R. (2008). Sequential expression of pluripotency markers during direct reprogramming of mouse somatic cells. Cell Stem Cell *2*, 151–159.

Fischedick, G., Klein, D.C., Wu, G., Esch, D., Hoing, S., Han, D.W., Reinhardt, P., Hergarten, K., Tapia, N., Scholer, H.R., et al. (2012). Zfp296 is a novel, pluripotent-specific reprogramming factor. PLoS One *7*, e34645.

Imamura, M., Miura, K., Iwabuchi, K., Ichisaka, T., Nakagawa, M., Lee, J., Kanatsu-Shinohara, M., Shinohara, T., and Yamanaka, S. (2006). Transcriptional repression and DNA hypermethylation of a small set of ES cell marker genes in male germline stem cells. BMC Dev. Biol. *6*, 34.

Johannesson, B., Sagi, I., Gore, A., Paull, D., Yamada, M., Golan-Lev, T., Li, Z., LeDuc, C., Shen, Y., Stern, S., et al. (2014). Comparable frequencies of coding mutations and loss of imprinting in human pluripotent cells derived by nuclear transfer and defined factors. Cell Stem Cell *15*, 634–642.

Kim, K., Doi, A., Wen, B., Ng, K., Zhao, R., Cahan, P., Kim, J., Aryee, M.J., Ji, H., Ehrlich, L.I., et al. (2010). Epigenetic memory in induced pluripotent stem cells. Nature *467*, 285–290.

Kim, S.M., Flasskamp, H., Hermann, A., Arauzo-Bravo, M.J., Lee, S.C., Lee, S.H., Seo, E.H., Lee, S.H., Storch, A., Lee, H.T., et al. (2014). Direct conversion of mouse fibroblasts into induced neural stem cells. Nat. Protoc. *9*, 871–881.

Ko, K., Tapia, N., Wu, G., Kim, J.B., Bravo, M.J., Sasse, P., Glaser, T., Ruau, D., Han, D.W., Greber, B., et al. (2009). Induction of pluripotency in adult unipotent germline stem cells. Cell Stem Cell *5*, 87–96.

Ko, K., Arauzo-Bravo, M.J., Kim, J., Stehling, M., and Scholer, H.R. (2010). Conversion of adult mouse unipotent germline stem cells into pluripotent stem cells. Nat. Protoc. *5*, 921–928.

Ko, K., Reinhardt, P., Tapia, N., Schneider, R.K., Arauzo-Bravo, M.J., Han, D.W., Greber, B., Kim, J., Kliesch, S., Zenke, M., et al. (2011). Brief report: evaluating the potential of putative pluripotent cells derived from human testis. Stem Cells *29*, 1304–1309.

Ko, K., Wu, G., Arauzo-Bravo, M.J., Kim, J., Francine, J., Greber, B., Muhlisch, J., Joo, J.Y., Sabour, D., Fruhwald, M.C., et al. (2012). Autologous pluripotent stem cells generated from adult mouse testicular biopsy. Stem Cell Rev. *8*, 435–444.

Ma, H., Morey, R., O'Neil, R.C., He, Y., Daughtry, B., Schultz, M.D., Hariharan, M., Nery, J.R., Castanon, R., Sabatini, K., et al. (2014). Abnormalities in human pluripotent cells due to reprogramming mechanisms. Nature *511*, 177–183.

Marthaler, A.G., Tiemann, U., Arauzo-Bravo, M.J., Wu, G., Zaehres, H., Hyun, J.K., Han, D.W., Scholer, H.R., and Tapia, N. (2013). Reprogramming to pluripotency through a somatic stem cell intermediate. PLoS One *8*, e85138.

Meissner, A., Gnirke, A., Bell, G.W., Ramsahoye, B., Lander, E.S., and Jaenisch, R. (2005). Reduced representation bisulfite sequencing for comparative high-resolution DNA methylation analysis. Nucleic Acids Res. *33*, 5868–5877.

Morimoto, H., Lee, J., Tanaka, T., Ishii, K., Toyokuni, S., Kanatsu-Shinohara, M., and Shinohara, T. (2012). In vitro transformation of mouse testis cells by oncogene transfection. Biol. Reprod. *86*, 148.

Polo, J.M., Liu, S., Figueroa, M.E., Kulalert, W., Eminli, S., Tan, K.Y., Apostolou, E., Stadtfeld, M., Li, Y., Shioda, T., et al. (2010). Cell type of origin influences the molecular and functional properties of mouse induced pluripotent stem cells. Nat. Biotechnol. *28*, 848–855.

Tachibana, M., Amato, P., Sparman, M., Gutierrez, N.M., Tippner-Hedges, R., Ma, H., Kang, E., Fulati, A., Lee, H.S., Sritanaudomchai, H., et al. (2013). Human embryonic stem cells derived by somatic cell nuclear transfer. Cell *153*, 1228–1238.

Tapia, N., and Schöler, H.R. (2010). p53 connects tumorigenesis and reprogramming to pluripotency. J. Exp. Med. *207*, 2045–2048.

Tiemann, U., Sgodda, M., Warlich, E., Ballmaier, M., Scholer, H.R., Schambach, A., and Cantz, T. (2011). Optimal reprogramming factor stoichiometry increases colony numbers and affects molecular characteristics of murine induced pluripotent stem cells. Cytometry A *79*, 426–435.

Tiemann, U., Marthaler, A.G., Adachi, K., Wu, G., Fischedick, G.U., Arauzo-Bravo, M.J., Scholer, H.R., and Tapia, N. (2014). Counteracting activities of OCT4 and KLF4 during reprogramming to pluripotency. Stem Cell Rep. *2*, 351–365.

Yoshimizu, T., Sugiyama, N., De Felice, M., Yeom, Y.I., Ohbo, K., Masuko, K., Obinata, M., Abe, K., Scholer, H.R., and Matsui, Y. (1999). Germline-specific expression of the Oct-4/green fluorescent protein (GFP) transgene in mice. Dev. Growth Differ. *41*, 675–684.

Zhao, Q., Wang, J., Zhang, Y., Kou, Z., Liu, S., and Gao, S. (2010). Generation of histocompatible androgenetic embryonic stem cells using spermatogenic cells. Stem Cells *28*, 229–239.